Small RNA and degradome deep sequencing reveal regulatory roles of miRNAs in response to *Sugarcane mosaic virus* infection on two contrasting sugarcane cultivars

Yuan Yuan [1,2†], Cuilin Huang[1†], Kaiyuan Pan[1], Wei Yao[1], Rui Xia[3], Muqing Zhang[1*]

[1] State Key Laboratory for Conservation and Utilization of Agro Bioresources; Guangxi Key Laboratory for Sugarcane Biology, Guangxi University, Nanning, 530005, China.

[2] Rubber Research Institute, Chinese Academy of Tropical Agricultural Science, Haikou, 570105, China

[3] State Key Laboratory for Conservation and Utilization of Subtropical Agro-Bioresources, College of Horticulture, South China Agricultural University, Guangzhou, 510642, China

[†] These authors contributed equally to the article.

[*] Corresponding author email: zmuqing@163.com

Abstract

MicroRNAs (miRNAs) play an essential regulatory role in plant–virus interaction. However, few studies have focused on the roles of miRNAs and their targets after *Sugarcane mosaic virus* (SCMV) infection in sugarcane. To address this issue, we conducted small RNA and degradome sequencing on two contrasting sugarcanes (SCMV-resistant FG1 and susceptible Badila) infected by SCMV at five time points. A total of 1578 miRNAs were profiled from 30 small RNA libraries, comprising 660 known miRNAs and 380 novel miRNAs. Differential expression analysis of miRNAs revealed that most were highly expressed during the SCMV exponential phase in Badila at 18h post-infection, with expression profiles positively correlated with virus replication dynamics, as observed through clustering. Analysis of degradome data indicated a higher number of differential miRNA targets in Badila compared to FG1 at 18 hours post-infection. Gene ontology (GO) enrichment analysis significantly enriched the stimulus-response pathway, suggesting negative regulatory roles to SCMV resistance. Specifically, miR160 upregulated expression patterns and validated in Badila through quantitative real-time PCR in the early stages of SCMV multiplication. Our research provides new insights into the dynamic response of plant miRNA and virus replication and contributes valuable information on the intricate interplay between miRNAs and SCMV infection dynamics.

Keywords: Sugarcane; Sugarcane mosaic virus; small RNA sequencing; degradome; miR160

Introduction

Sugarcane (*Saccharum officinarum*) is a significant sugar crop worldwide. *Sugarcane mosaic virus* (SCMV), a dominant pathogen of sugarcane mosaic disease causing severe economic losses, is a single-stranded sense RNA virus belonging to the genus *Potyvirus*, family Potyviridae (Lakshmanan et al., 2005; Viswanathan and Balamuralikrishnan, 2005). SCMV damages cell chloroplasts and reduces photosynthesis, restricting plant growth during viral multiplication (Gao et al., 2011; Xie et al., 2021). During the extensive encounters against viruses, plants have evolved various antiviral mechanisms, of which RNA silencing-mediated viral resistance is one of the most concerning mechanisms. MicroRNA is an essential small silencing RNA involved in host antimicrobial immunity in eukaryotic organisms (Guo et al., 2019). However, the response of miRNAs for SCMV infection in the early multiplication remains unknown in sugarcane.

sRNA-mediated silencing was first discovered in plant anti-virus research, which protects the plant immune system against infection, maintains genomic stability, and regulates growth and development (Baulcombe and David, 2004; Ding and Shou-Wei, 2010). sRNA commonly inhibits the expression or translation of target genes by guiding complementary mRNA or viral RNA with the degradation, thereby silencing target genes and regulating their expression (Csorba et al., 2009). On the other hand, viruses have evolved RNA silencing suppressors that affect RISC assembly and subsequent mRNA degradation in the arms race between plants and viruses, which is for evading the host immune response and enhancing their pathogenic ability (Hu et al., 2018; Mengistu and Tenkegna, 2021).

MicroRNA is a single-stranded, non-coding small RNA molecule. It comprises approximately 21-23 nucleotides produced through the cleavage of endogenous transcripts containing stem-loop structure by a Dicer-like enzyme. The mechanism of plant miRNA is complex, involving various RNA polymerase enzymes and nucleases, as well as numerous stages from transportation to processing. Gene encoding miRNA in the nucleus is transcribed by RNA polymerase II to form a primary transcript of pri-miRNA. Then, the pri-miRNA is processed into a stem loop-structured precursor

miRNA (pre-miRNA) by endonuclease Dicer-like (DCL) cleavage and released into small double-stranded RNAs (dsRNAs). The miRNA duplex is further cleaved to mature miRNA in the cytoplasm by interaction with DCL, initiating the formation of the RNA-induced silencing complex (RISC). RISCs are guided to degrade target mRNA with argonaute protein (AGO) through complementary pairing (Yekta et al., 2004; Akbar et al., 2022). During the RNA silencing antiviral process, in addition to miRNAs generated from endogenous plant RNA, the host processes viral RNA into siRNAs, known as virus-derived siRNA (Ding and Voinnet, 2007; Liu et al., 2021). Antiviral silencing mediated by viral siRNA plays a vital role in plant resistance to virus infection. These siRNAs can associate with host proteins to form the RNA-induced silencing complex (RISC), which directly targets and cleaves viral genomic RNA that is complementary to the siRNAs, thereby silencing the target viral genes (Ding and Shou-Wei, 2010; Zhao et al., 2021).

MiRNAs mediate the response of plant-pathogen interaction. The miRNA expression rapidly responds in the host plant after pathogen infection, causing changes in downstream target gene expression, thereby regulating the disease resistance of the plant host. At present, many miRNAs have been identified in plants. They can be used as an essential transcriptional regulation factor to regulate the immune response triggered by pathogen-associated molecular patterns and effectors. For example, deep miRNA sequencing of rice blast sensitive and resistant lines has identified some miRNAs with expression patterns related to disease resistance genes, and overexpression of miR160a and miR398b showed enhanced resistance in rice (Li et al., 2013). miR393 regulates lectin receptor-like kinases associated with LPS perception in *Arabidopsis thaliana* and enhances basal resistance (Djami-Tchatchou and Dubery, 2019). However, miRNAs also play a negative regulatory role in plant disease resistance. In tomatoes, miR482 and miR5300 were identified to suppress NB-LRR domain protein that confers resistance to *Fusarium oxysporum* (Ouyang et al., 2014). Furthermore, miR398b negatively regulates cotton immune responses to *Verticillium dahliae via* multiple targets involved in reactive oxygen species (ROS) regulation and homeostasis (Miao et al., 2022). A mechanism has been revealed in rice to enhance

antiviral defense by inhibiting miRNA528 that binds to L-ascorbic acid oxidase (AO) mRNA in *ago18* null mutants, resulting in a decreased accumulation of ROS and negative regulation of rice virus resistance (Wu et al., 2017).

Our study focused on Fuoguo1 (FG1) derived from susceptible Badila, which maintains high resistance to sugarcane mosaic disease. To investigate the role of miRNA during the SCMV infection process, we performed small RNA and degradome sequencing on SCMV-infected leaves from two contrasting cultivars (SCMV-resistant FG1 and susceptible Badila) at five-time points (0h, 6h, 18h, 48h, and 192h), post SCMV inoculation. The expression profile of miRNA was deciphered in response to SCMV infection with a comparative analysis between the resistant and susceptible sugarcane genotypes. Our study revealed that miRNA might affect SCMV virus replication by regulating targeted genes related to stimulus-response. This study provides new insights into the role of miRNA in plant–virus interaction.

Results

Global small RNA profiling under SCMV infection

FG1 (Fuguo 1) was a registered sugarcane variety resistant to sugarcane mosaic virus (SCMV). The accumulation level of SCMV RNA exhibited significant differences in virus replication dynamics between resistant and susceptible sugarcane at different time points following infection. FG1 remained at a lower level, whereas the susceptible sugarcane Badila showed exponential amplification of SCMV, especially at 18 hours post-infection (Fig. 1A). To explore the role of sugarcane small RNAs (sRNAs) in the infection of *sugarcane mosaic virus*, we investigated the dynamic changes of small RNA in resistant and susceptible sugarcane. Thirty libraries generated 646,799,799 raw reads by small RNA sequencing. After quality control through removing low-quality reads and adapters, 41,046,287 clean reads were obtained. Then, the sRNA reads contaminated with chloroplast genome (cpGenome) and ribosomal RNA (rRNA) sequences were filtered out through sequence alignment, as shown in Table S1. The results showed that approximately 20% of the sequenced reads originated from the cp genome, and 10% were aligned to rRNA. After filtering non-nuclear small RNAs, clean data were mapped to the FG1 genome (unpublished) with a high alignment rate, an average of 91% (Table S1). The length distribution of sRNA revealed that most reads are concentrated in the range of 21-24 nucleotide (nt) (Fig. 1B). Among these, the

highest number of reads corresponded to 24-nt length, mainly phasiRNAs (phased, secondary, minor interfering RNAs), followed by miRNAs at 21-nt length. Overall, Badila exhibited more sRNA reads than FG1, with more reads in the length range of miRNAs (21-22 nt) in Badila than in FG1 (Fig. 1B), indicating a higher expression abundance of miRNAs in susceptible lines.

During the assembly process, sRNA reads of 21-22nt were selected for miRNA prediction. All information on genome annotation was placed in the miRNA of the file (Table S2). The result showed that 3,158 miRNA genes were identified (618 unique sequence miRNAs), of which 1,579 were expressed as mature. The identified miRNA repertoire consisted of 660 known miRNAs, 380 novel miRNAs, and 538 potential miRNAs (Fig. 1C). The correlation-coefficient matrix plot showed that the sample from Badila at 18 hours post-infection exhibited a lower correlation with the other samples, indicating that the miRNA expression in Badila-18h might possess a distinctive characteristic (Fig. 1D). Principal component analysis (PCA) demonstrated that two samples, Badila-6h and Badila-18h, maintained significant divergence when compared to the other samples. This finding suggested a more significant variation in miRNA expression levels during these two periods (Fig. 1E).

SCMV-derived siRNA and SCMV replication dynamics

To demonstrate the expression profile of siRNAs in sugarcane, we used the SCMV genome as a reference and performed filtered alignment to obtain siRNA reads. The expression trends of siRNA count in each sample were shown in Fig. 2A. Notably, siRNA counts were relatively low in FG1 but significantly higher in Badila, especially at 18h post-inoculation. The expression profile of SCMV-derived siRNA displayed the SCMV replication dynamics. To further understand the siRNA sequences, a distribution plot of all reads from the Badila on the SCMV genome was generated (Fig. 2B). The results revealed two enriched clusters located on the P3 and CP gene sequences, possibly related to the expression abundance of these genes.

Dominant expression of miRNA in susceptible Badila

To explore the differences in miRNA expression between SCMV-resistant and susceptible sugarcane, we performed differential expression analysis of miRNAs in FG1 and Badila at different time points. The results revealed 566 differentially expressed miRNAs across five points (Table S3). Venn diagram analysis showed that unique differential miRNAs dominated at the 18h and 192h post-inoculation (Fig. 3A).

Additionally, we identified seven miRNAs that displayed differential expression across all time points, namely miRN18b, miRN18d, miRN54b, miRN54a, miRN18a, miRN18c, and miRN54d. Interestingly, the upregulated differentially expressed miRNAs in Badila were consistently more abundant than in FG1 at each time point, especially at 18h when viral replication peaked. The differential expression of these miRNAs in Badila was five times higher than FG1 (Fig. 3B). Furthermore, the expression heatmap was evident that miRNAs in the Badila-18h sample exhibited significantly higher expression levels (Fig. 3C). Using the sRNAminer software, we predicted nearly 59,705 candidate target genes (including alleles) for all the differentially expressed miRNAs (Table S4). GO enrichment analysis revealed that these genes were predominantly involved in cellular processes (GO:0009987) and metabolic processes (GO:0019748) and associated with molecular functions such as nucleic acid binding (GO:0005488) and catalytic activity (GO:0003824). Moreover, numerous genes were involved in biological regulation and stimulus-response processes.

MiRNA exhibits a unique expression pattern associated with SCMV replication dominant miRNA expression in susceptible Badila.

MiRNA is an essential component of the transcriptional regulatory network. The expression of miRNA is dynamically regulated, which means that the expression levels of miRNA can vary at different time points or under different environmental conditions. The k-means clustering was performed to investigate the temporal dynamic of miRNA for resistant and susceptible sugarcane after SCMV infection. The miRNA expression patterns were categorized into four clusters, with cluster 1 encompassing the largest number of miRNAs and exhibiting the most significant differential expression change (Fig. 4A, Table S5). Cluster 1, containing 388 miRNAs, shared a typical expression pattern in which genes maintained low expression levels throughout various time points in FG1 but showed a rapid transcriptional upregulation at 18 hours post-infection in the susceptible Badila. Remarkably, this expression pattern displayed a significant positive correlation with the replication profile of SCMV in both samples. Among cluster 1, miRNAs were highly expressed at Badila-18h, the most significant differences including miR171 and miR160 families (Fig. S1, Table S6). The miRN54a was overexpressed explicitly in Badila and not expressed in FG1.

Identification of miRNA target genes through degradome sequencing

We identified a dominant miRNA cluster whose expression trend is associated with viral replication, suggesting the possibility of their crucial role in facilitating viral replication in the host. Based on differently expressed miRNA sequences, over 16,076 candidate target genes were identified using degradation group prediction (category < 3). At the critical time point of 18 hours after SCMV infection, the number of target genes regulated by cluster 1 miRNAs exhibited a significant difference, in which 931 target genes were identified in FG1, while 2,305 target genes were identified in Badila (Table S7). The count in Badila is approximately 2.5 times higher than in FG1 (Fig. 4A), indicating more mRNA silencing events in Badila-18h, characterized by a higher abundance of miRNA target genes. Comparing the overlap of target genes between FG1 and Badila at the critical period (18h), the Venn diagram showed that 449 genes were shared, but a more significant proportion of target genes were exclusive to Badila (Fig. 4B). We further explored the functional implications of these differentially regulated target genes. GO enrichment analysis revealed a significantly higher number of genes in Badila compared to FG1, displaying a notable enrichment in the biological process associated with stimulus-response (GO:0050896) and cellular components related to the plastid (GO:0009536) (Fig. 4C).

Our findings indicated that miRNAs were predominantly upregulated in the susceptible Badila, while miRNA expression in FG1 remained stable at different time points after SCMV treatment. miRNAs displayed significantly induced in response to SCMV infection. The expression pattern of miRNA was consistent with the viral replication curve, suggesting a close association between miRNA and viral replication. Identified miRNA and their target genes predominantly function in stimulus-response and might be involved in the SCMV replication dynamic in susceptible Badila.

Constructing miRNA-genes regulatory network

MiRNA actively responding to SCMV replication in susceptible Badila showed that their target genes were significantly enriched in a biological process-related stimulus response. A total of 633 target genes are involved in stimulus-response and corresponding different expression miRNA. The functional annotation showed that most of these genes regulated biological processes (Table S8). Domain analysis showed that the top families included protein kinase, small heat shock protein Hsp20, calmodulin, bZIP, and MYB transcription factor families (Fig. S2). A multi-omics

integrative analysis combined with small RNA sequencing and degradation sequencing was performed. Firstly, we obtained these target protein interaction networks (PPI) using the STRING database (https://string-db.org/). Next, regulatory relationships were determined between miRNAs and corresponding target genes based on degradome. We reconstructed the regulatory network with the fold difference of miRNA expression at 18h. We displayed the miRNA-gene interaction network by Cytoscape software (Fig. 5). This network showed 33 different expression miRNAs targeting 160 genes involved in stimulus-response, including several core miRNAs. miR5079 with maximum node degree regulated the most target genes. The most considerable fold change was found in miR160, showing the most significant expression difference at 18h post-infection. We identified some high-frequency node target genes involved in stimulus-response, such as encoding chaperone protein CLPB1, heat shock protein HSP81-1, and calcium-binding protein CML32 and CML24. Meanwhile, some target genes were involved in defense response, including transcription factor TGAL6 and NAC048, E3 ubiquitin-protein NPR2 and NPR3, cinnamoyl-CoA reductase-like SNL6. These genes were negatively regulated by highly expressed miRNAs in Badila, which might be the reason for attenuated defense against SCMV infection.

Verification of differential miRNAs and target genes

We further validated the highest expression differences with miRNA160. Seventy miR160 families were identified, including two differentially expressed miRNA subtypes in sugarcane. The first subtype expressed the same miRNA sequence "GCGTGCGAGGTGCCAAGCATGG," consisting of miR160d-Known-3p-star, miR160e-Known-3p-star, miR160f-Known-3p-star, miR160g-Known-3p-star, miR160h-Known-3p-star, and miR160i-Known-3p-star. miR160d was considered the representative miRNA of this subtype. The second subtype expressing a miRNA sequence "GCGTGCAAGGAGCCAAGCATG" included miR160ad-Probable-5p-mature, miR160ae-Known-3p-star, miR160af-Known-3p-star, miR160ag-Known-3p-star, miR160ah-Known-3p-star, and miR160ai-Known-3p-star. miR160a was considered the representative miRNA of the second subtype. The expression of these miRNAs was verified through the alignment of small RNA sequencing data using IGV-sRNA software (https://gitee.com/CJchen/IGV-sRNA). The validation results showed significant differences in read count for miR160d, miR160e, and miR160h of the first

subtype. In contrast, only miR160ae of the second subtype exhibited differential expression in response to resistance or susceptibility to SCMV (Fig. 6A).

Furthermore, qPCR was used to validate the differential miRNA expression. The qPCR results showed consistent relative expression levels and expression trends for three miRNA sequences. Both miR160d and miR160ae were found to have significantly higher expression levels in Badila at 18 hours post-SCMV infection (Fig. 6B). Additionally, a target gene with a repetitive leucine-rich sequence, encoded by the LRR gene (SoZg.04B006970.1), was identified among the degradation targets of miR160d/e/h. The qRT-PCR depicted the expression trend of LRR, suggesting the negative expression correlation between LRR and miR160d (Fig. 6C).

Discussion

Plants inevitably encounter various biotic stresses throughout their growth, prompting the development of adaptive mechanisms during their long-term evolution. MicroRNA (miRNAs) are pivotal in regulating plant development and responses to environmental stresses, including interaction with viruses (Raza et al., 2023) (Mengistu and Tenkegna, 2021). Sugarcane, a globally significant crop for sugar production and a promising green carbon source in biomass (Karp et al., 2022), needs a comprehensive understanding of miRNA-mediated regulatory mechanisms in response to viral infections. Hence, investigating how resistant sugarcane variety FG1 and susceptible Badila respond to Sugarcane mosaic virus (SCMV) becomes crucial for understanding the detailed regulatory network involved. This research enhances our understanding of miRNA-generated responses in sugarcane and contributes to the strategies for enhancing resistance against SCMV infections.

Small RNA molecules, particularly microRNAs (miRNAs), play an essential role in plant defense against viral infections (Lu et al., 2008; Mengistu and Tenkegna, 2021). Specific miRNAs target viral genomes or plant host genes associated with viral infections, thereby regulating the antiviral response of plants and enhancing immune capabilities (Kong et al., 2022). Notably, recent studies have revealed that viruses possess mechanisms to evade the host plant immune response during plant-virus interaction by modulating the expression of plant miRNAs. Plant miRNAs could counteract viral infections through negative regulation (Wu et al., 2015) and are

profoundly involved in this defense mechanism against viral invasions.

Upon invading a host, the virus spreads and replicates throughout the plant to induce disease. During this stage, a dynamic interaction occurs between the virus and host, with the virus striving to establish infection while the host endeavors to resist it. Our research findings showed that resistant sugarcane FG1 retained a low viral load. Contradictorily, the replication curve of the SCMV infection on the Badila leaves showed inadequate resistance to SCMV during the confrontation of the virus and host cells. The observed transition trend of virus replication from exponential expansion to stabilization was likely caused by the movement of SCMV in the Badila leaves after infection.

In this study, we investigated the expression differences of miRNAs in resistant sugarcane FG1 and susceptible Badila at different time points post-SCMV infection by small RNA sequencing and degradome sequencing techniques. Notably, a higher number of small RNA reads were generated in Badila after infection, as compared to FG1, and the assembled miRNA reads also showed a similar abundance advantage. The analysis highlighted the primary contributions derived from the rapid expansion of miRNA in Badila following SCMV infection. Additionally, the expression profile of miRNAs post-SCMV infection revealed characteristic differences in the Badila-18h post-infection, as elucidated through differential expression and sample correlation analysis.

Combined with the absolute quantification and transcriptional expression analysis of SCMV, as mentioned earlier, the 18h post-infection was identified as the viral replication phase. During this phase, there was notable and abrupt enhancement of miRNA expression. Similar phenomena have been reported in the response of rice to rice stripe virus (RSV) infection, where the expression level of miR160, miR166, miR167, miR171, and miR396 families increased (Du et al., 2011). Our research specifically identified a significant responsiveness of miR160 to SCMV. The miR160 family is involved in diverse functions, initially identified in *Arabidopsis* as regulators of auxin response factors (Rhoades et al., 2002). The down-regulation of OsmiR160 targeting OsARF18 resulted in growth and development defects in rice and caused

auxin signaling (Huang et al., 2016). Ectopic expression of miR160 induced super-sensitivity to auxin in soybeans, among other effects (Turner et al., 2013). Furthermore, miR160 played a crucial regulatory role in biotic stress, demonstrating positive feedback during the response to cassava anthracnose disease (Pinweha et al., 2015). Previous research showed that miR160 played a crucial role in plant defense against viruses and insects such as cucumber mosaic virus and rice stripe virus (Bazzini et al., 2007; Du et al., 2011; Kundu et al., 2017). This regulatory role is possibly exerted through the induction of RNA silencing pathway components.

Among the target genes of miR160, seven genes encoding the CAB2R protein (including alleles or homologous genes) are located at the chloroplast thylakoid membrane, associated with the light-harvesting complex (LHC), and function as light receptors tightly linked to chloroplast development. Besides their role as the site of photosynthesis, chloroplasts are crucial components of plant defense responses and actively participate in plant-virus interactions. Notably, chloroplasts are the primary target for successfully infecting plant viruses into hosts. High expression of miR160 exacerbated the inhibitory regulation of the CABR2 gene, possibly resulting in a weakening of chloroplast defense. Furthermore, we also identified the candidate target gene LRR (Leucine-Rich Repeat) of miR160, which exhibits a negative regulatory expression pattern with miR160. However, this gene has been relatively understudied regarding its function, and regulatory mechanisms require further investigation.

Based on integrative analysis using multiple omics data, we constructed a miRNA-mRNA regulatory network involving stress response and displayed several core miRNAs. The noteworthy findings on miR5079 involved in heat stress tolerance have been reported (Mangrauthia et al., 2017). Our research unveils novel facts about miR5079, elucidating its potential functions related to virus response. miR167 has been recognized as a significant contributor to resistance against maize chlorotic mottle virus (MCMV) through the Zma-miR167-ARF3/30-PAO1 signaling pathway (Liu et al., 2022). Intriguingly, our research diverges from previous investigations, as we observed the induction of miR167 by *Sugarcane mosaic virus* (SCMV). Contrary to its role in MCMV resistance in maize, miR167 did not exhibit such a response to SCMV,

suggesting that the functions of miR167 might vary in response to distinct viruses or hosts.

Further investigations are required to better understand specific functions associated with identified target genes. Some target genes were identified within this regulatory network as involved in plant defense. NPR2 and NPR3, belonging to the BTB/POZ domain and ankyrin repeat-containing protein, are reportedly involved in the defense response against bacterial blight disease in rice (Yuan et al., 2007). The transcription factors involved in defense response, such as TGAL6 (Fitzgerald et al., 2005) and NAC048 (Nakashima et al., 2007), were found to be negatively regulated by differentially expressed miRNAs.

In summary, many miRNAs were positively expressed with SCMV replication, forming a distinct cluster. The functions of the miRNA clustered target genes, through degradome sequencing data, are significantly enriched in stimulus-response, suggesting a regulatory mechanism where SCMV induces the expression of miRNAs, which negatively regulate stress response genes involved in defense mechanisms. This regulatory process might attenuate SCMV resistance, enabling the virus to colonize the host successfully. These findings highlight the involvement of miRNAs in the regulatory mechanism of SCMV virus infection and provide a molecular foundation for understanding host defense against viral infections.

Material and method

Plant materials and treatment

Sugarcane (*Saccharum officinarium* L.), resistant genotype Fuguo 1 (FG1), is registered in the Ministry of Agriculture and Rural Affairs of China Trial Registry (registration number: GPD Sugarcane (2022) 450016), sustaining high resistance against SCMV infection, and obtained by somatic mutation of susceptible cultivar Badila (Nanning, Guangxi, China). Stable growth conditions were supplied at 24-28 °C with 16:8h of light/dark photoperiod. The first leaf, one-month-old (4/5-leaf stage) and grown above the ligule, was mechanically infected with sap (at 6 pm). Sap was prepared using crude extract of SCMV-infected leaves with phosphate buffer (PB), stained using 80 mesh quartz. Inoculation was performed using fingers which lightly reciprocate

friction five times. Leaves were wrapped with fresh film to maintain humidity. After infection, sampling was collected at different time points (0h, 6h, 18h, 48h, and 192h). Each leaf was cut 15 cm, which distributed three inoculation sites, with each about 1 cm wide. A total of 30 samples from five points were collected, each from Badila and FG1. Two replicates from each sample were collected for further analysis. A total of 30 sRNA and 10 degradome libraries were constructed. Three sRNA library samples (biological replicates) from the same time point were merged into one degradome library.

Small RNA and degradome library construction

Construction of a small RNA library. Total RNA was extracted using TRIzol reagent (Invitrogen, Carlsbad, CA, USA), according to the manufacturer's guidelines. The RNA concentration and purity were quantified using NanoDrop ND-1000 (NanoDrop, Wilmington, DE, USA). The integrity of RNA was evaluated by Bioanalyzer 2100 (Agilent, CA, USA) and verified by agarose gel electrophoresis. The experimental procedure followed the standard steps provided by Illumina company, including library preparation and sequencing experiments. A small RNA sequencing library was obtained using TruSeq ™ Small RNA Sample Prep Kits (Illumina, San Diego, USA). The constructed library was sequenced using Illumina Hiseq2500 with a single-end reading length of 1 × 50bp.

Construction of degradome cDNA library. Poly(A) RNA was purified from plant total RNA (20ug) using poly-T oligo-attached magnetic beads in two rounds of purification for each sample. The RNA ligase ligated the adapters to the 5' end of the 3' cleavaged mRNA. Reverse transcription was performed to synthesize the first strand of cDNA with a 3′-adapter random primer. Following the vendor's recommended protocol, the 50bp single-end sequencing was performed on an Illumina Hiseq 2500 (LC Bio, China). We have constructed 30 small RNA libraries and a degradome cDNA library, respectively. Constructions of libraries and RNA sequencing were performed by the Hangzhou Lianchuan Biotechnology Co., Ltd (Hangzhou, Zhejiang, China).

MiRNA prediction and quantification

The raw sequencing data was assembled and analyzed using sRNAminer software (https://github.com/kli28/sRNAminer). The FG1 genome was used as the reference genome (unpublished). The currently known miRNA was downloaded from the database miRbase (ftp://mirbase.org/pub/mirbase/CURRENT/mature.fa.gz). The small RNA quality was controlled by filtering-related databases from NCBI, including all ribosomal RNA (rRNA) and chloroplast genome (cpGenome) databases. sRNAseqAdapterPrediction program was used to predict the adapter for clean_data. The small RNA sequencing data adapter was removed by sRNAseqAdapterRemover and deduplicated by sRNAseqCollasper. Ribosomal RNA and cpGenome databases were mapped to filter contamination of rRNA and organelle genome reads. Filtering reads were mapped to the FG1 genome by sRNAseqAlignmentFormater. Based on the miRbase database, the identification of miRNA used miRNAminerCLI (--matureColIndex 6 --starColIndex 7 --starAbundanceIndex 11). SRNAQuantify quantified the abundance of miRNA expression, and standardized expression information (RPTM) was obtained. The prediction of small RNA (siRNA) produced by SCMV was the same as above, except that the SCMV genome (NC_003398.1) was used as the reference genome.

miRNA expression analysis

Sample correlation coefficient analysis and principal component analysis (PCA) were performed by R package corrplot (Wei and Simko, 2021) and vegan (Dixon, 2003). Differential expression analysis of miRNA was conducted between FG1 and Badila at the same time points by DESeq2 (Love et al., 2014) and identified differential miRNA (fold change >1, p-value <0.05). Venn diagrams were drawn by Tbtools (Chen et al., 2020), displaying the similarities and differences of differentially expressed genes at different time points. All heatmaps were generated with the R package heatmap (Zhang et al., 2016). Using sRNAminer (TargetSoPipe) to predict candidate target genes of miRNAs based on FG1 genome data. The expression trend cluster for differential miRNA was analyzed using the R package Mfuzz (Kumar and M, 2007). The GO annotation for each gene comes from the FG1 genome functional annotation. GO enrichment evaluation is performed using TBtools and followed by visualization using

the R package ggplot2 (Ginestet, 2011). All GO categories with p-values<1e-05 were considered enrichment options.

Identification of miRNA target genes using degradome sequencing

Degradome sequencing raw data was executed for quality control by removing the adapter from sRNAminer (sRNAseqAdapterPrediction and sRNAseqAdapterRemover) packages. Target genes of differential miRNA analysis were identified in degradome sequencing data using CleaveLand4 (v4.5, https://github.com/MikeAxtell/CleaveLand4/archive/refs/heads/master.zip) (Addo-Quaye et al., 2009) with default parameters. Detailed information about each target gene corresponding to a miRNA was generated (Table S9). The CleaveLand4 software only predicted one miRNA at a time. The first used type 1 model parameters that align gradient data align small RNA queries and analyze (- e -u -n). Then, the degradation group file remained freezing, and different miRNA sequences were performed to identify the type 2 model (- d - u - n).

qRT-RCR analysis

We assessed the relative expression level of the *CP* gene to indicate the accumulation level of SCMV RNA using qRT-PCR. The tailing-based method was used to quantify miRNA. RNA samples were reverse transcribed to obtain cDNA with Poly (A) using a microRNA one-step cDNA synthesis kit (Takara 638315), following the kit protocol. The real-time qPCR with three biological replications was performed with SYBR green on the Roche Lightcyler® 480 instrument using the SYBR fluorescence quantification method (Takara, RR820A). The U6 gene was selected as miRNA reference genes. The forward primers were designed on the miRNA sequence, and a few nucleotides were added at the 5' end according to the specific requirements. The reagent kit provides reverse primers of miRNA, but the sequence was unpublished because of intellectual property. MRNA quantification referenced the previous qRT-RCR protocol (Yuan et al., 2021). The primer sequences are shown in Table S10.

Data availability statement

The original contributions presented in the study are publicly available. This raw data

was available at https://submit.ncbi.nlm.nih.gov/subs/sra/SUB14082371.

Funding

This research was financially supported by the China Agricultural Research System of MOF and MARA (CARS170109) and the Guangxi Key Project of the Scientific and Technological Department (Guike AA22117001).

Author contributions

MQZ conceived and designed the project. YY assembled and analyzed the data. CLH performed sugarcane treatment and the experiments. KYP detected the level of SCMV accumulation. WY assisted sugarcane materials. RX contributed technical software support. YY and CLH wrote the manuscript with contributions from MQZ.

Conflict of Interest Statement

The authors declare that the research was conducted without any commercial or financial relationships that could be construed as a potential conflict of interest.

Literature Cited

Addo-Quaye, C., Miller, W., and Axtell, M.J. 2009. CleaveLand: a pipeline for using degradome data to find cleaved small RNA targets. Bioinformatics 25:130-131.

Akbar, S., Wei, Y., and Zhang, M.-Q. 2022. RNA Interference: Promising Approach to Combat Plant Viruses. International Journal of Molecular Sciences 23:5312.

Baulcombe, and David. 2004. RNA silencing in plants. Nature 431:356-363.

Bazzini, A.A., Hopp, H.E., Beachy, R.N., and Asurmendi, S. 2007. Infection and coaccumulation of tobacco mosaic virus proteins alter microRNA levels, correlating with symptoms and plant development. Proceedings of the National Academy of Sciences of the United States of America 104:12157-12162.

Chen, C., Chen, H., Zhang, Y., Thomas, H.R., Frank, M.H., He, Y., and Xia, R. 2020. TBtools: An Integrative Toolkit Developed for Interactive Analyses of Big Biological Data. Molecular Plant 13:1194-1202.

Csorba, T., Pantaleo, V., and Burgyán, J. 2009. RNA silencing: an antiviral mechanism. Advances in Virus Research 75:35-71.

Ding, and Shou-Wei. 2010. RNA-based antiviral immunity. Nature Reviews Immunology 10:632-644.

Ding, S.W., and Voinnet, O. 2007. Antiviral immunity directed by small RNAs. Cell 130:413-426.

Dixon, P. 2003. VEGAN, a package of R functions for community ecology. Journal of Vegetation Science 14:927-930.

Djami-Tchatchou, A.T., and Dubery, I.A. 2019. miR393 regulation of lectin receptor-like kinases associated with LPS perception in Arabidopsis thaliana. Biochemical and Biophysical Research Communications 513:88-92.

Du, P., Wu, J., Zhang, J., Zhao, S., Zheng, H., Gao, G., Wei, L., and Li, Y. 2011. Viral Infection Induces Expression of Novel Phased MicroRNAs from Conserved Cellular MicroRNA Precursors. PLOS Pathogens 7:e1002176.

Fitzgerald, H.A., Canlas, P.E., Chern, M.S., and Ronald, P.C. 2005. Alteration of TGA factor activity in rice results in enhanced tolerance to Xanthomonas oryzae pv. oryzae. The Plant Journal: for cell and molecular biology 43:335-347.

Gao, B., Cui, X.W., Li, X.D., Zhang, C.Q., and Miao, H.Q. 2011. Complete genomic sequence analysis of a highly virulent isolate revealed a novel strain of Sugarcane mosaic virus. Virus Genes 43:390-397.

Ginestet, C. 2011. ggplot2: Elegant Graphics for Data Analysis. Journal of the Royal Statistical Society 174:245-246.

Guo, Z., Li, Y., and Ding, S.W. 2019. Small RNA-based antimicrobial immunity. Nature reviews. Immunology 19:31-44.

Hu, F., Lei, R., Deng, Y.F., Wang, J., Li, G.F., Wang, C.N., Li, Z.H., and Zhu, S.F. 2018. Discovery of novel inhibitors of RNA silencing suppressor P19 based on virtual screening. RSC advances 8:10532-10540.

Huang, J., Li, Z., and Zhao, D. 2016. Deregulation of the OsmiR160 Target Gene OsARF18 Causes Growth and Developmental Defects with an Alteration of Auxin Signaling in Rice. Sci Rep 6:29938.

Karp, S.G., Burgos, W.J.M., Vandenberghe, L.P.S., Diestra, K.V., Torres, L.A.Z., Woiciechowski, A.L., Letti, L.A.J., Pereira, G.V.M., Thomaz-Soccol, V., Rodrigues, C., de Carvalho, J.C., and Soccol, C.R. 2022. Sugarcane: A Promising Source of Green Carbon in the Circular Bioeconomy. Sugar

Tech 24:1230-1245.

Kong, X., Yang, M., Le, B.H., He, W., and Hou, Y. 2022. The master role of siRNAs in plant immunity. Mol Plant Pathol 23:1565-1574.

Kumar, L., and M, EF 2007. Mfuzz: a software package for soft clustering of microarray data. Bioinformatics 2:5-7.

Kundu, A., Paul, S., Dey, A., and Pal, A. 2017. High throughput sequencing reveals modulation of microRNAs in Vigna mungo upon Mungbean Yellow Mosaic India Virus inoculation highlighting stress regulation. Plant Science: an international journal of experimental plant biology 257:96-105.

Lakshmanan, P., Geijskes, R.J., Aitken, K.S., Grof, C.L.P., Bonnett, G.D., and Smith, G.R. 2005. Sugarcane biotechnology: The challenges and opportunities. In Vitro Cellular & Developmental Biology - Plant 41:345-363.

Li, Y., Lu, Y.-G., Shi, Y., Wu, L., Xu, Y.-J., Huang, F., Guo, X.-Y., Zhang, Y., Fan, J., Zhao, J.-Q., Zhang, H.-Y., Xu, P.-Z., Zhou, J.-M., Wu, X.-J., Wang, P.-R., and Wang, W.-M. 2013. Multiple Rice MicroRNAs Are Involved in Immunity against the Blast Fungus Magnaporthe oryzae. Plant Physiology 164:1077-1092.

Liu, P., Zhang, X., Zhang, F., Xu, M., Ye, Z., Wang, K., Liu, S., Han, X., Cheng, Y., Zhong, K., Zhang, T., Li, L., Ma, Y., Chen, M., Chen, J., and Yang, J. 2021. A virus-derived siRNA activates plant immunity by interfering with ROS scavenging. Molecular Plant 14:1088-1103.

Liu, X., Liu, S., Chen, X., Prasanna, B.M., Ni, Z., Li, X., He, Y., Fan, Z., and Zhou, T. 2022. Maize miR167-ARF3/30-polyamine oxidase 1 module-regulated H2O2 production confers resistance to maize chlorotic mottle virus. Plant Physiol 189:1065-1082.

Love, M.I., Huber, W., and Anders, S. 2014. Moderated estimation of fold change and dispersion for RNA-seq data with DESeq2. Genome Biology 15:550.

Lu, Y.D., Gan, Q.H., Chi, X.Y., and Qin, S. 2008. Roles of microRNA in plant defense and virus offense interaction. Plant Cell Reports 27:1571-1579.

Mangrauthia, S.K., Bhogireddy, S., Agarwal, S., Prasanth, V.V., Voleti, S.R., Neelamraju, S., and Subrahmanyam, D. 2017. Genome-wide changes in microRNA expression during short and prolonged heat stress and recovery in contrasting rice cultivars. Journal of Experimental Botany 68:2399-2412.

Mengistu, A.A., and Tenkegna, T.A. 2021. The role of miRNA in plant-virus interaction: a review. Molecular Biology Reports 48:2853-2861.

Miao, Y., Chen, K., Deng, J., Zhang, L., Wang, W., Kong, J., Klosterman, S.J., Zhang, X., Aierxi, A., and Zhu, L. 2022. miR398b negatively regulates cotton immune responses to Verticillium dahliae via multiple targets. The Crop Journal 10:1026-1036.

Nakashima, K., Tran, L.S., Van Nguyen, D., Fujita, M., Maruyama, K., Todaka, D., Ito, Y., Hayashi, N., Shinozaki, K., and Yamaguchi-Shinozaki, K. 2007. Functional analysis of a NAC-type transcription factor OsNAC6 involved in abiotic and biotic stress-responsive gene expression in rice. The Plant Journal: for cell and molecular biology 51:617-630.

Ouyang, S., Park, G., Atamian, H.S., Han, C.S., Stajich, J.E., Kaloshian, I., and Borkovich, KA 2014. MicroRNAs suppress NB domain genes in tomatoes that confer resistance to Fusarium oxysporum. PLoS Pathog 10:e1004464.

Pinweha, N., Asvarak, T., Viboonjun, U., and Narangajavana, J. 2015. Involvement of miR160/miR393 and their targets in cassava responses to anthracnose disease. J Plant Physiol 174:26-35.

Raza, A., Charagh, S., Karikari, B., Sharif, R., Yadav, V., Mubarik, M.S., Habib, M., Zhuang, Y., Zhang, C., Chen, H., Varshney, RK, and Zhuang, W. 2023. miRNAs for crop improvement. Plant Physiology and Biochemistry 201:107857.

Rhoades, M.W., Reinhart, B.J., Lim, L.P., Burge, C.B., Bartel, B., and Bartel, D.P. 2002. Prediction of plant microRNA targets. Cell 110:513-520.

Turner, M., Nizampatnam, N.R., Baron, M., Coppin, S., Damodaran, S., Adhikari, S., Arunachalam, S.P., Yu, O., and Subramanian, S. 2013. Ectopic expression of miR160 results in auxin hypersensitivity, cytokinin hyposensitivity, and inhibition of symbiotic nodule development in soybeans. Plant Physiol 162:2042-2055.

Viswanathan, R., and Balamuralikrishnan, M. 2005. Impact of mosaic infection on growth and yield of sugarcane. Sugar Tech 7:61-65.

Wei, T.-y., and Simko, V. (2021). R package 'corrplot': Visualization of a Correlation Matrix (Version 0.92).

Wu, J., Yang, R., Yang, Z., Yao, S., Zhao, S., Wang, Y., Li, P., Song, X., Jin, L., Zhou, T., Lan, Y., Xie, L., Zhou, X., Chu, C., Qi, Y., Cao, X., and Li, Y. 2017. ROS accumulation and antiviral defense control by microRNA528 in rice. Nature Plants 3:16203.

Wu, J., Yang, Z., Wang, Y., Zheng, L., Ye, R., Ji, Y., Zhao, S., Ji, S., Liu, R., Xu, L., Zheng, H., Zhou, Y., Zhang, X., Cao, X., Xie, L., Wu, Z., Qi, Y., and Li, Y. 2015. Viral-inducible Argonaute18 confers broad-spectrum virus resistance in rice by sequestering a host microRNA. eLife 4.

Xie, J., Jiang, T., Li, Z., Li, X., Fan, Z., and Zhou, T. 2021. Sugarcane mosaic virus remodels multiple intracellular organelles to form genomic RNA replication sites. Archives of Virology 166:1921-1930.

Yekta, S., Shih, I.H., and Bartel, D.P. 2004. MicroRNA-directed cleavage of HOXB8 mRNA. Science (New York, N.Y.) 304:594-596.

Yuan, Y., Yang, X., Feng, M., Ding, H., Khan, M.T., Zhang, J., and Zhang, M. 2021. Genome-wide analysis of R2R3-MYB transcription factors family in the autopolyploid Saccharum spontaneum: an exploration of dominance expression and stress response. BMC Genomics 22:622.

Yuan, Y., Zhong, S., Li, Q., Zhu, Z., Lou, Y., Wang, L., Wang, J., Wang, M., Li, Q., Yang, D., and He, Z. 2007. Functional analysis of rice NPR1-like genes reveals that OsNPR1/NH1 is the rice orthologue conferring disease resistance with enhanced herbivore susceptibility. Plant Biotechnology Journal 5:313-324.

Zhang, X., Yao, X., Qin, C., Luo, P., and Zhang, J. 2016. Investigation of the molecular mechanisms underlying metastasis in prostate cancer by gene expression profiling. Experimental and Therapeutic Medicine 12:925-932.

Zhao, S., Wu, Y., and Wu, J. 2021. Arms race between rice and viruses: a review of viral and host factors. Current Opinion in Virology 47:38-44.

Figure legends

Fig. 1 Characterization of small RNAs in sugarcane. A, The accumulation level of SCMV RNA for SCMV-resistant FG1 and susceptible Badila after infection. **B,** Length distribution of the small RNAs from the 30 libraries of SCMV-resistant FG1 and susceptible Badila. **C,** types of identified miRNA. **D,** Heatmap of correlation matrix. **E,** Principal component analysis (PCA).

Fig. 2 Map of SCMV-derived siRNA. A SCMV-derived siRNA displays the dynamics of SCMV on two sugarcane lines; **B,** the distribution of siRNA within Badila on the SCMV genome.

Fig. 3 Differential expression analysis of miRNA. A Venn diagram of differential miRNA between FG1 and Badila at each stage. **B,** the up- or down-regulated miRNA by FG1 compared with Badila; **C,** Heatmap of differentially expressed miRNA; **D,** GO enrichment analysis of target genes predicted by miRNA.

Fig. 4 Clustering of miRNA expression trends and functional analysis of target genes. A, K-means clustering showing the miRNA expression profiles. **B,** the number of differential miRNA target genes based on degradome 18 hours after infection. **C,** Venn of target genes. **D,** GO enrichment analysis of miRNA target genes.

Fig. 5 Regulatory networks of miRNA-mRNA in response to SCMV. The gradient-colored sphere represented the fold change of miRNA expression. The blue sphere represented the target genes related to stress response based on the degradation group. The size of the sphere represents the number of nodes. The PPI interaction between target genes provided a framework for constructing regulatory networks. The multiple lines between two genes were due to the characteristics of multiple alleles in sugarcane.

Fig. 6 The significant differential expression of miR160 between resistant and susceptible sugarcane. A, Genome browser showing the alignment of miR160 reads at 18h after infection. **B** and **C,** Results of qRT-PCR showing accumulation profile of miR160 and targets among the times points after infection. REL (relative expression level) was calculated using FG1 without treatment (FG1-0h) as a control.

Supplementary files

Figure S1 Heatmap of differential expression miRNA in Badila at 18h.

Figure S2 Distribution of target gene domains.

Table S1 Summary data of small RNA sequencing from the 30 libraries.

Table S2 MiRNA gff annotation.

Table S3 The list of differentially expressed miRNAs by Badila vs FG1.

Table S4 The list of miRNA-predicted target genes.

Table S5 The list of miRNAs with four expression clusters.

Table S6 The list of significantly differentially expressed miRNAs in cluster 1.

Table S7 Genes targeting differential miRNA by identifying degradome sequencing at 18h.

Table S8 The annotation of target genes involved in stimulus-response.

Table S9 Target genes of differentially expressed miRNAs identified through degradome sequencing.

Table S10 Primers applied in this study.

A

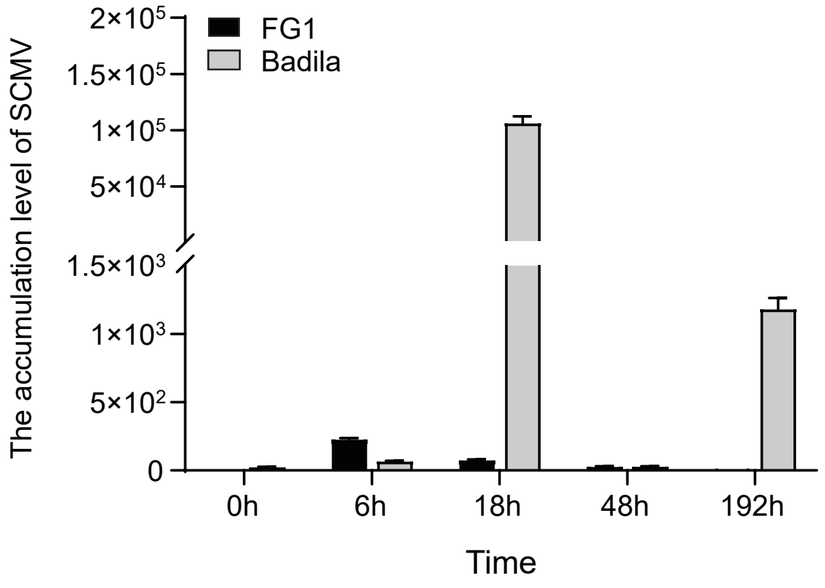
FG1
Badila
The accumulation level of SCMV
2×10^5
1.5×10^5
1×10^5
5×10^4
1.5×10^3
1×10^3
5×10^2
0
0h
6h
18h
48h
192h
Time

B

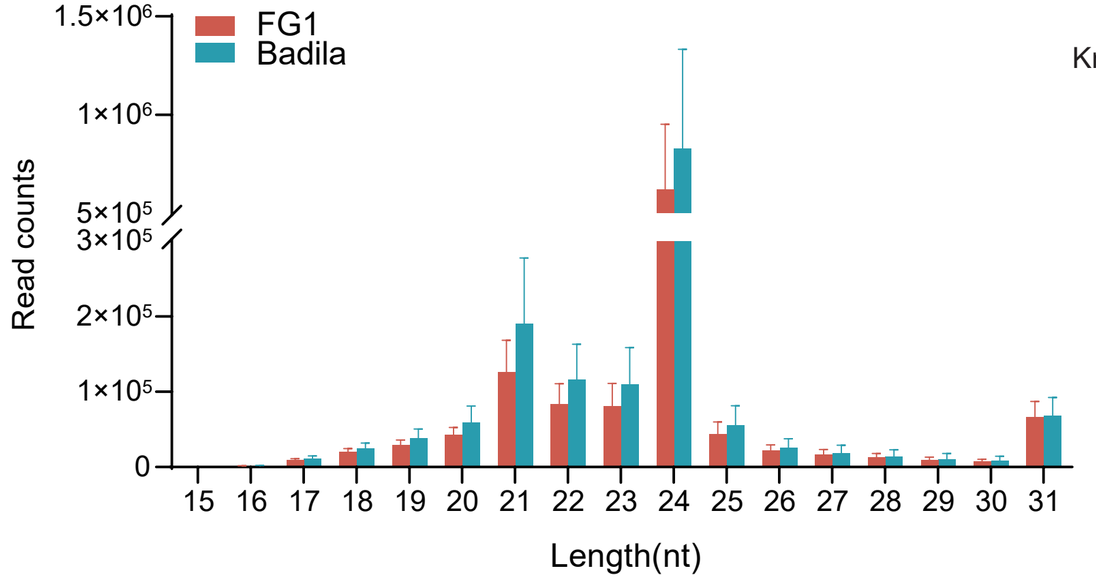
FG1
Badila
Read counts
1.5×10^6
1×10^6
5×10^5
3×10^5
2×10^5
1×10^5
0
15
16
17
18
19
20
21
22
23
24
25
26
27
28
29
30
31
Length(nt)

C

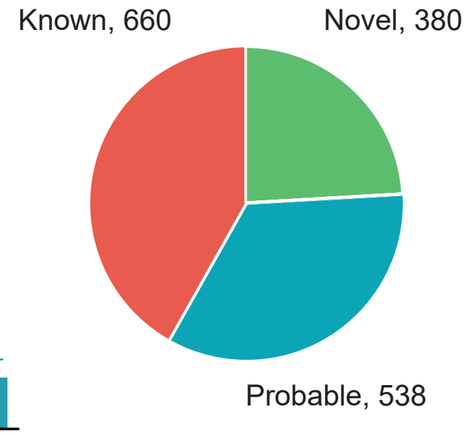
Known, 660
Novel, 380
Probable, 538

D

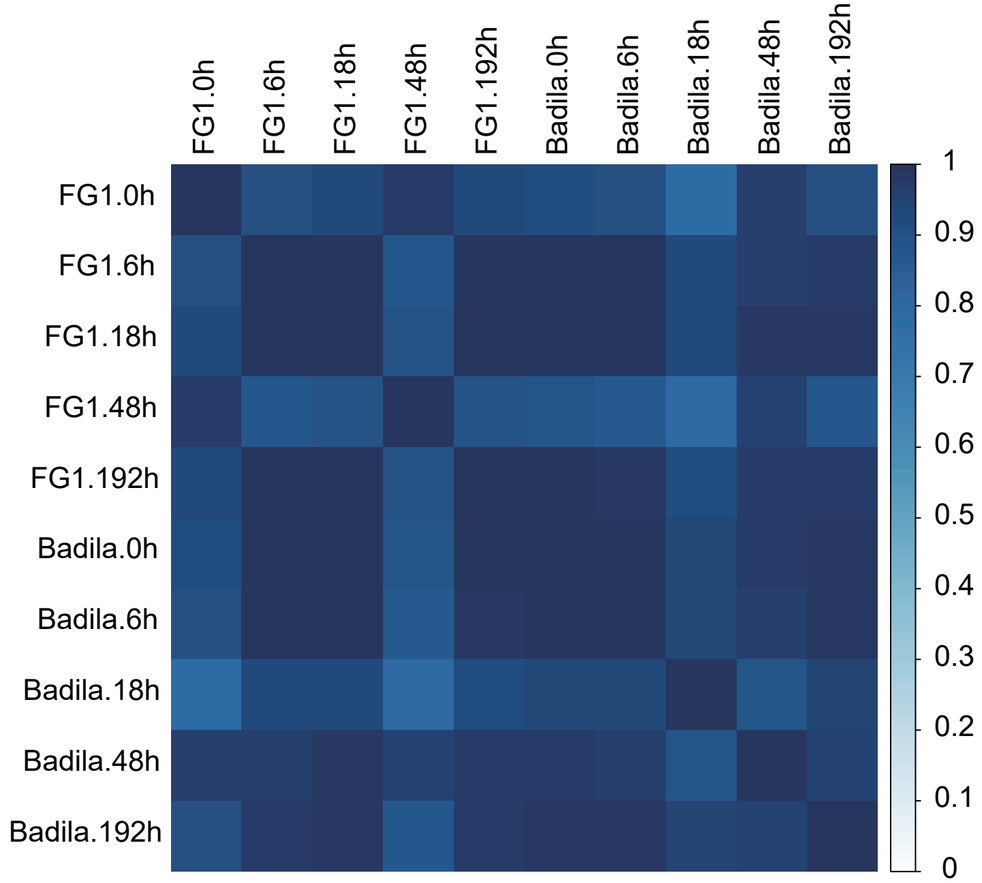
FG1.0h
FG1.6h
FG1.18h
FG1.48h
FG1.192h
Badila.0h
Badila.6h
Badila.18h
Badila.48h
Badila.192h
1
0.9
0.8
0.7
0.6
0.5
0.4
0.3
0.2
0.1
0

E

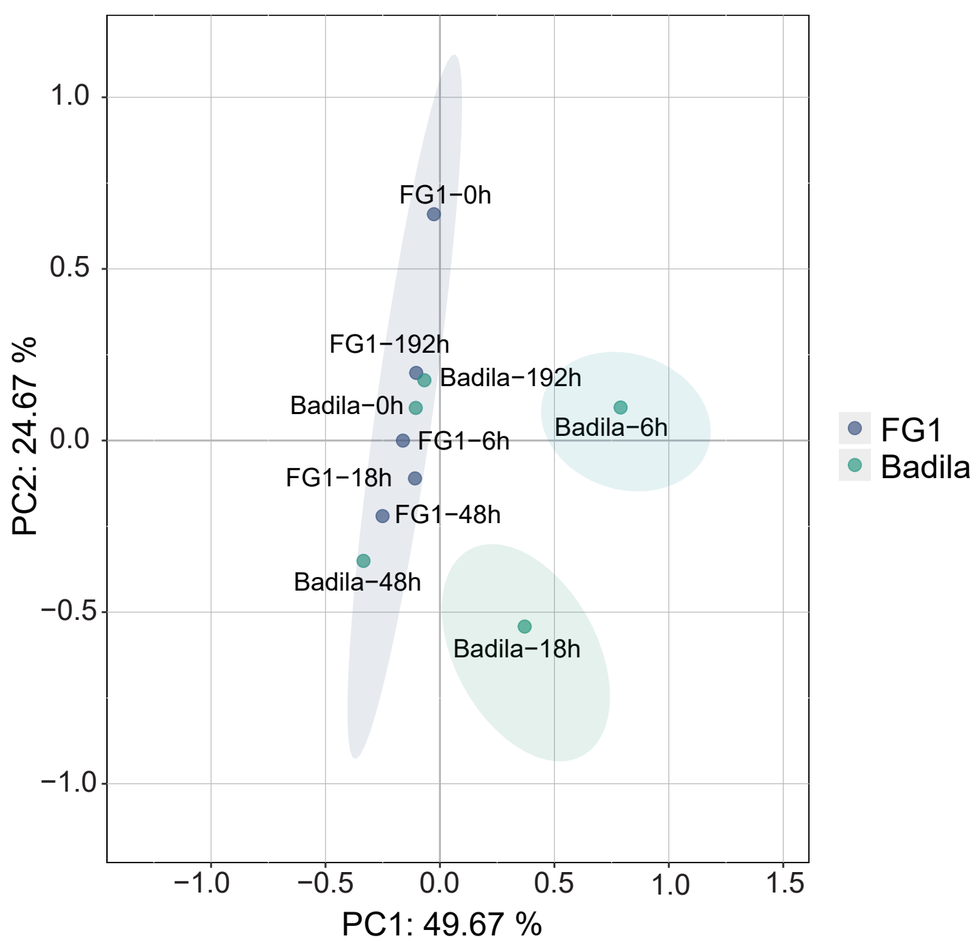
FG1−0h
FG1−192h
Badila−192h
Badila−0h
Badila−6h
FG1−6h
FG1−18h
FG1−48h
Badila−48h
Badila−18h
PC2: 24.67 %
PC1: 49.67 %
FG1
Badila

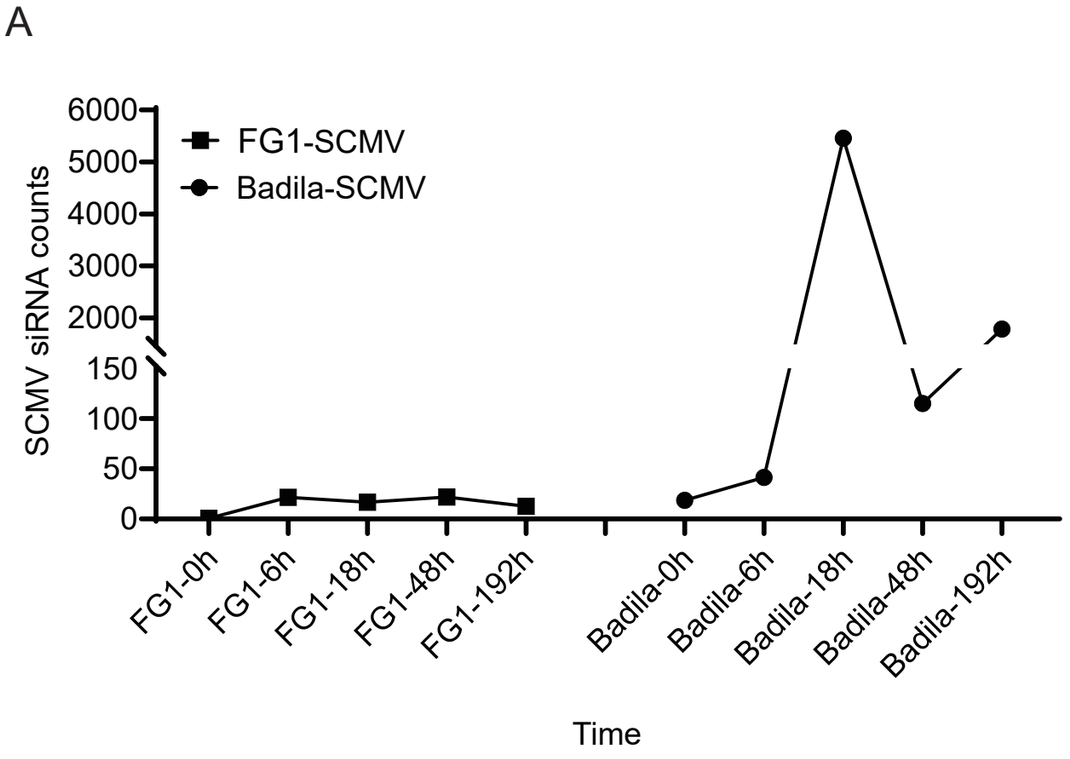
A
6000
5000
4000
3000
2000
150
100
50
0
SCMV siRNA counts
FG1-SCMV
Badila-SCMV
FG1-0h
FG1-6h
FG1-18h
FG1-48h
FG1-192h
Badila-0h
Badila-6h
Badila-18h
Badila-48h
Badila-192h
Time

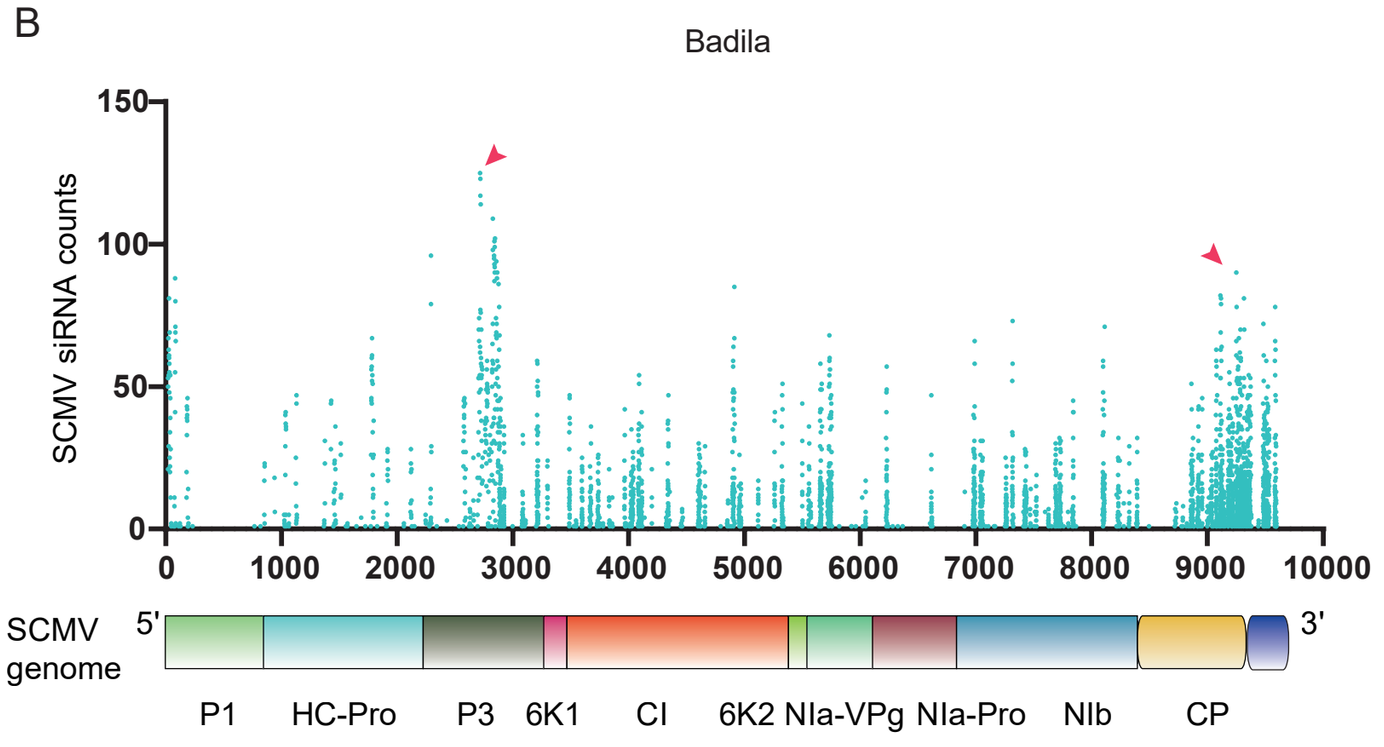
B
Badila
150
100
50
0
SCMV siRNA counts
0
1000
2000
3000
4000
5000
6000
7000
8000
9000
10000
SCMV genome
5'
3'
P1
HC-Pro
P3
6K1
CI
6K2
NIa-VPg
NIa-Pro
NIb
CP

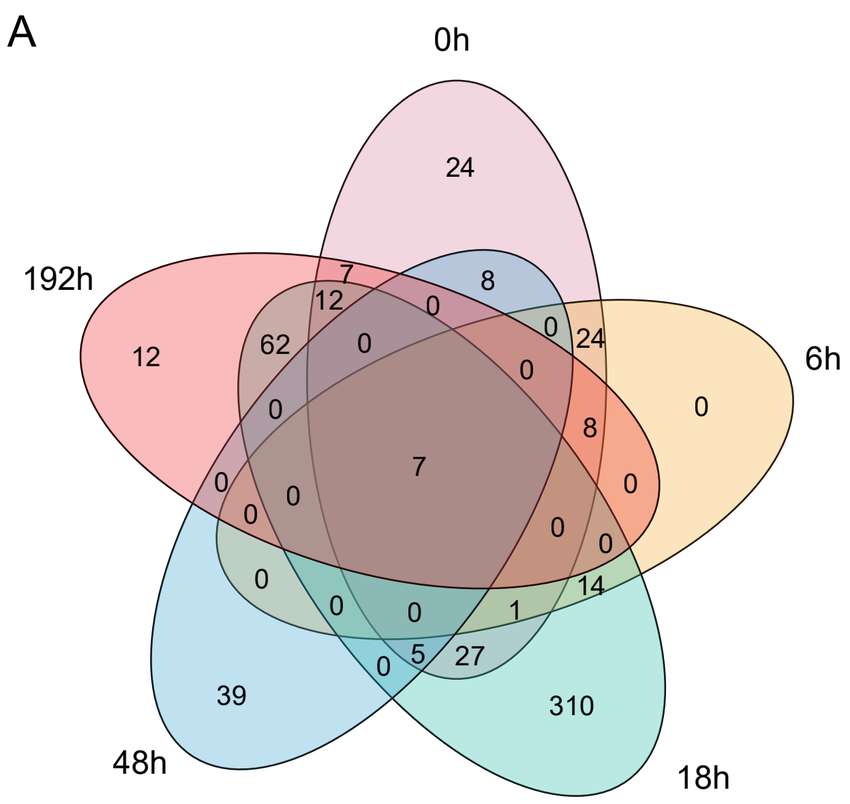
A
0h
6h
18h
48h
192h
24
12
62
7
12
0
8
0
24
0
0
0
8
0
0
0
0
0
0
0
0
0
14
0
0
1
0
5
27
39
310
7

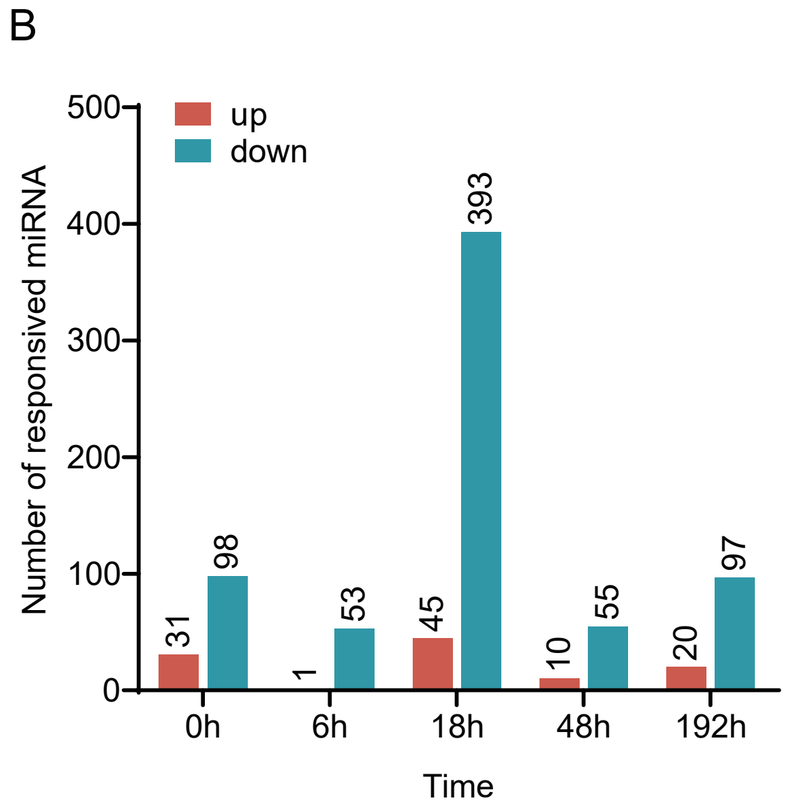
B
Number of responsived miRNA
up
down
500
400
300
200
100
0
31
98
1
53
45
393
10
55
20
97
0h
6h
18h
48h
192h
Time

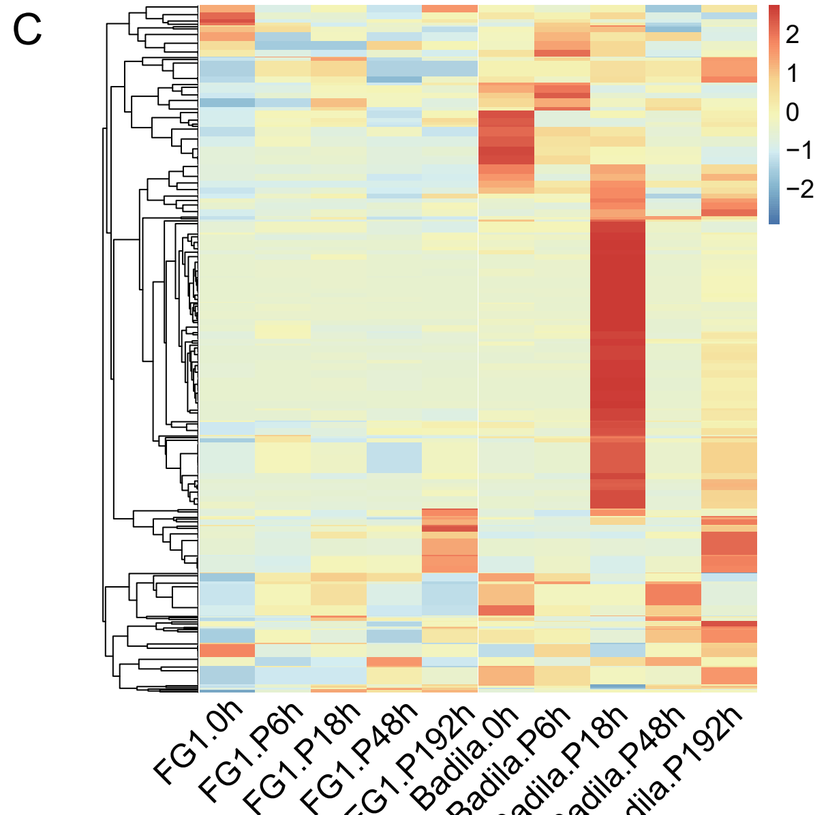
C
2
1
0
−1
−2
FG1.0h
FG1.P6h
FG1.P18h
FG1.P48h
FG1.P192h
Badila.0h
Badila.P6h
Badila.P18h
Badila.P48h
Badila.P192h

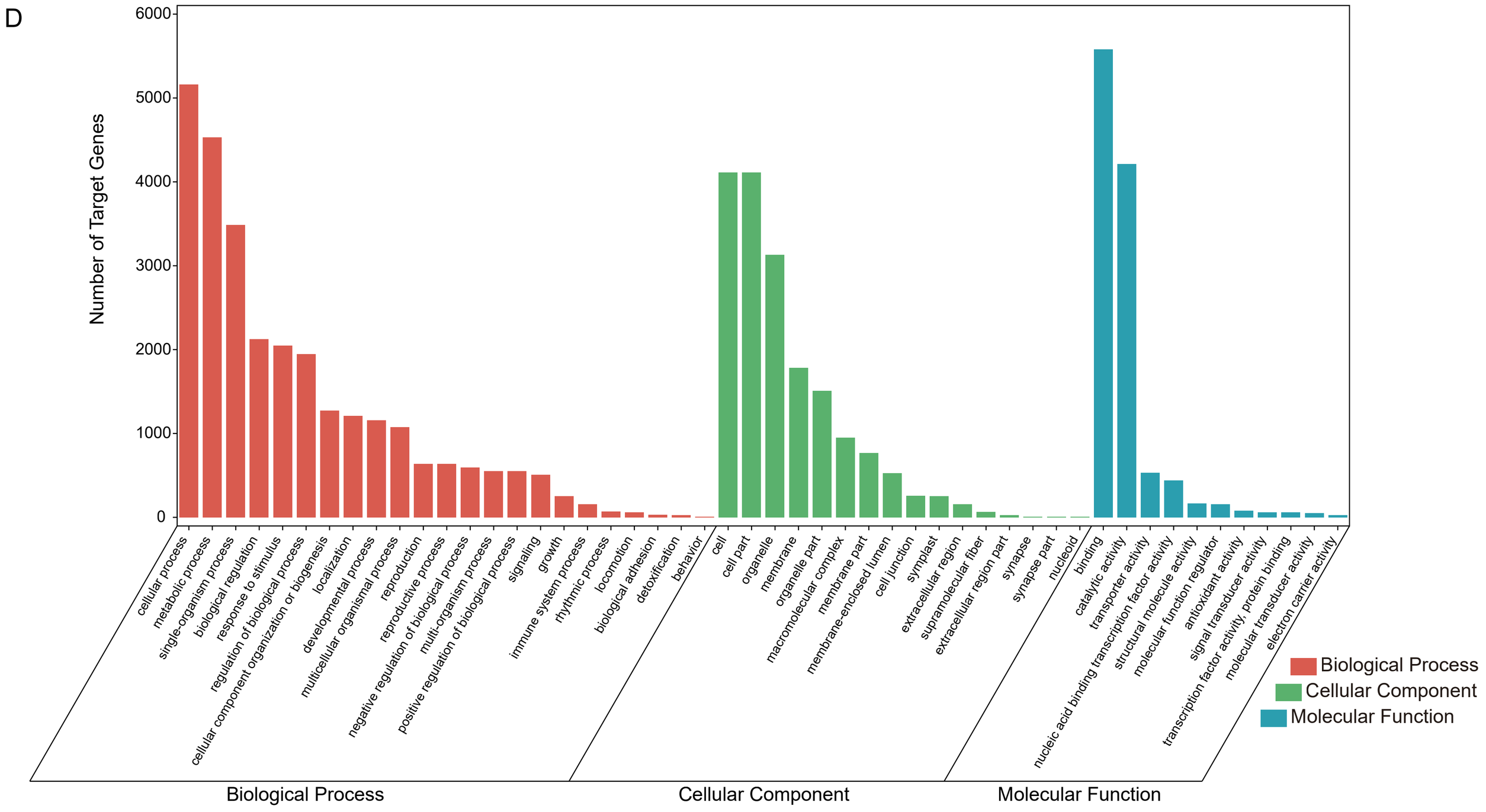
D
Number of Target Genes
6000
5000
4000
3000
2000
1000
0
cellular process
metabolic process
single-organism process
biological regulation
response to stimulus
regulation of biological process
cellular component organization or biogenesis
localization
developmental process
multicellular organismal process
reproduction
reproductive process
negative regulation of biological process
multi-organism process
positive regulation of biological process
signaling
growth
immune system process
rhythmic process
locomotion
biological adhesion
detoxification
behavior
cell
cell part
organelle
membrane
organelle part
macromolecular complex
membrane part
membrane-enclosed lumen
cell junction
symplast
extracellular region
supramolecular fiber
extracellular region part
synapse
synapse part
nucleoid
binding
catalytic activity
transporter activity
nucleic acid binding transcription factor activity
structural molecule activity
molecular function regulator
antioxidant activity
signal transducer activity
transcription factor activity, protein binding
molecular transducer activity
electron carrier activity
Biological Process
Cellular Component
Molecular Function
Biological Process
Cellular Component
Molecular Function

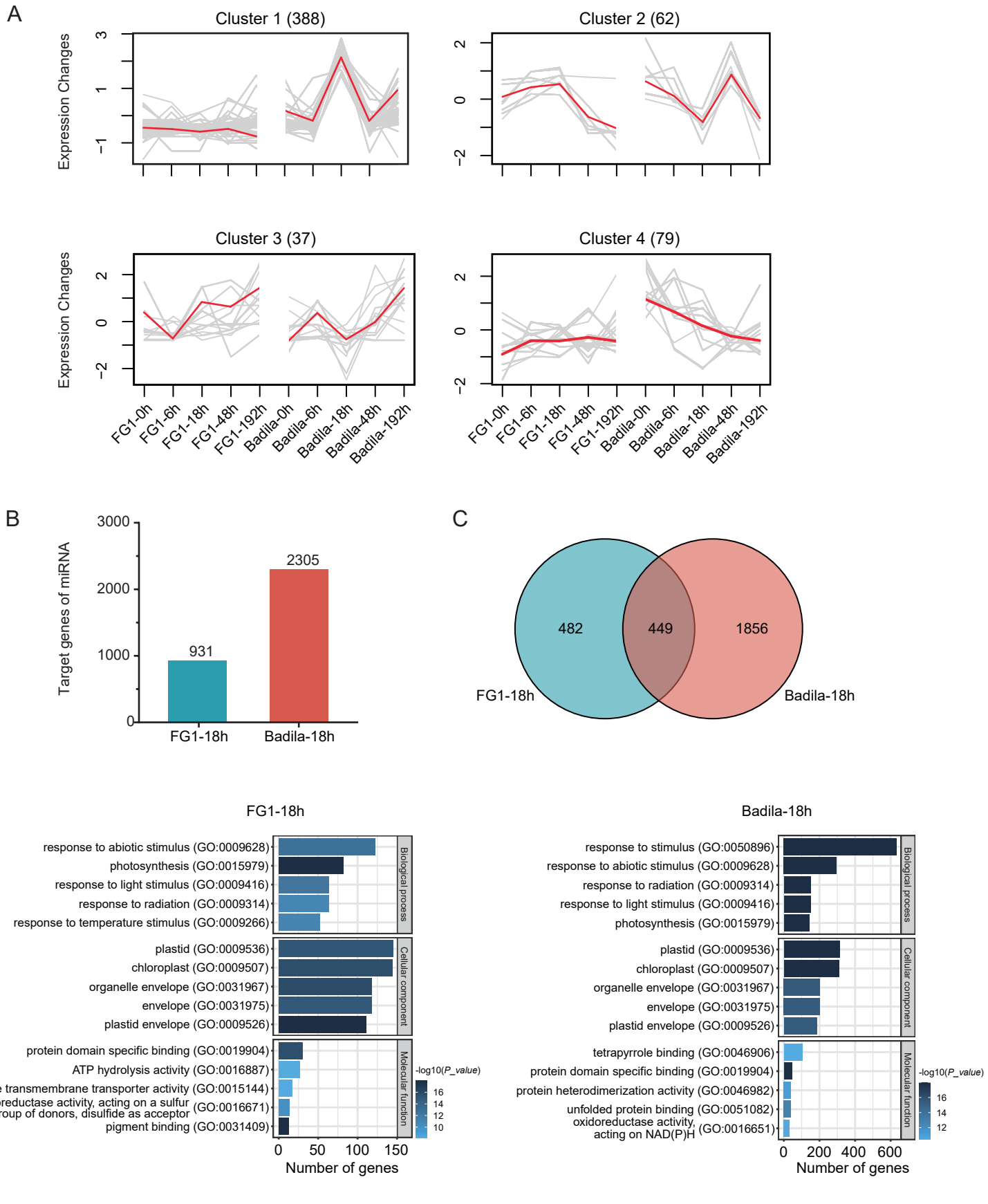
A
Cluster 1 (388)
Cluster 2 (62)
Cluster 3 (37)
Cluster 4 (79)
Expression Changes
FG1-0h
FG1-6h
FG1-18h
FG1-48h
FG1-192h
Badila-0h
Badila-6h
Badila-18h
Badila-48h
Badila-192h
B
Target genes of miRNA
3000
2000
1000
0
931
2305
FG1-18h
Badila-18h
C
482
449
1856
FG1-18h
Badila-18h
D
FG1-18h
Badila-18h
Goterm
response to abiotic stimulus (GO:0009628)
photosynthesis (GO:0015979)
response to light stimulus (GO:0009416)
response to radiation (GO:0009314)
response to temperature stimulus (GO:0009266)
response to stimulus (GO:0050896)
plastid (GO:0009536)
chloroplast (GO:0009507)
organelle envelope (GO:0031967)
envelope (GO:0031975)
plastid envelope (GO:0009526)
protein domain specific binding (GO:0019904)
ATP hydrolysis activity (GO:0016887)
carbohydrate transmembrane transporter activity (GO:0015144)
oxidoreductase activity, acting on a sulfur group of donors, disulfide as acceptor (GO:0016671)
pigment binding (GO:0031409)
tetrapyrrole binding (GO:0046906)
protein heterodimerization activity (GO:0046982)
unfolded protein binding (GO:0051082)
oxidoreductase activity, acting on NAD(P)H (GO:0016651)
Biological process
Cellular component
Molecular function
-log10(P_value)
Number of genes

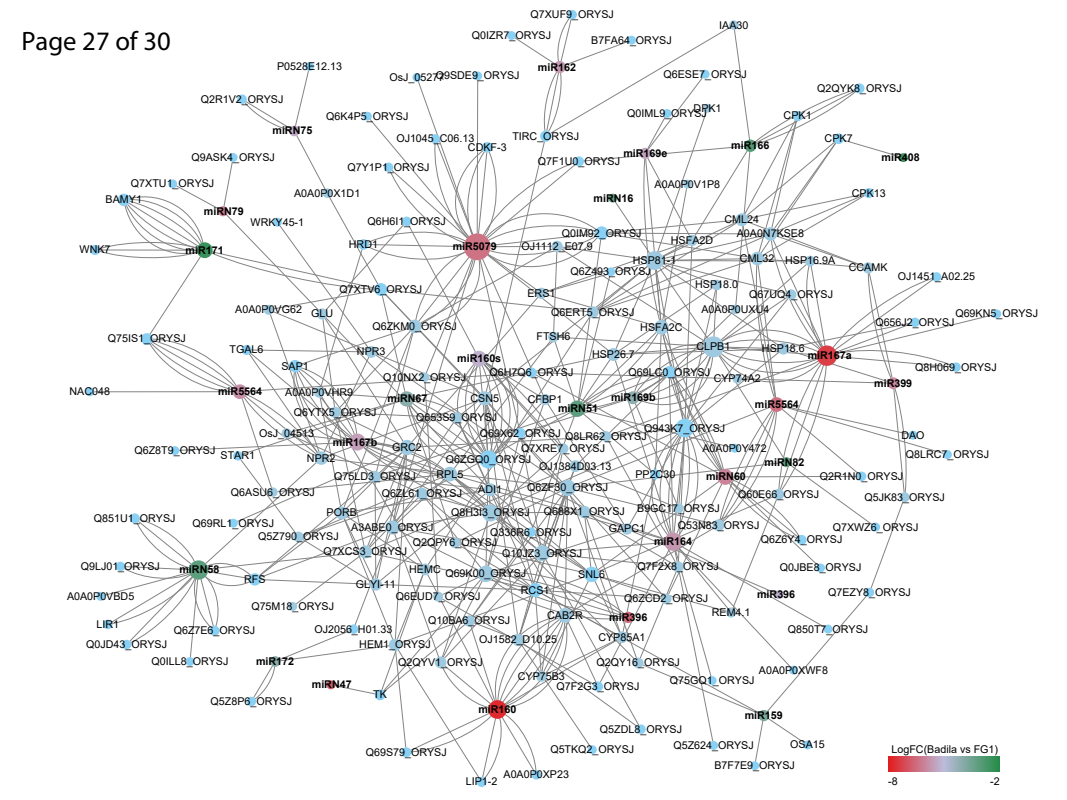
Q7XUF9_ORYSJ
IAA30
Q0IZR7_ORYSJ
B7FA64_ORYSJ
P0528E12.13
miR162
OsJ_052709
Q9SDE9_ORYSJ
Q6ESE7_ORYSJ
Q2QYK8_ORYSJ
Q2R1V2_ORYSJ
miRN75
Q6K4P5_ORYSJ
Q0IML9_ORYSJ
PDK1
CPK1
OJ1045_C06.13
TIRC_ORYSJ
CPK7
miR408
CDKF-3
miR169e
miR166
Q9ASK4_ORYSJ
Q7Y1P1_ORYSJ
Q7F1U0_ORYSJ
Q7XTU1_ORYSJ
A0A0P0V1P8
BAMY1
A0A0P0X1D1
miRN16
CPK13
miRN79
WRKY45-1
Q6H6I1_ORYSJ
CML24
HRD1
miR5079
OJ1112_E07.9
Q0IMQ2_ORYSJ
HSFA2D
A0A0N7KSE8
WNK7
miR171
Q6Z493_ORYSJ
HSP81-1
CML32
HSP16.9A
CCAMK
OJ1451_A02.25
Q7XTV6_ORYSJ
ERS1
HSP18.0
Q67UQ4_ORYSJ
A0A0P0VG62
GLU
Q6ERT5_ORYSJ
A0A0P0UXU4
Q69KN5_ORYSJ
Q75IS1_ORYSJ
Q6ZKM0_ORYSJ
FTSH6
HSFA2C
Q656J2_ORYSJ
TGAL6
NPR3
HSP26.7
GLPB1
HSP18.6
miR167a
SAP1
miR160s
Q8H069_ORYSJ
Q10NX2_ORYSJ
Q6H7Q6_ORYSJ
Q69LC0_ORYSJ
CYP74A2
miR399
NAC048
miR5564
A0A0P0VHR9
miRN67
CSN5
CFBP1
miR169b
miRN51
Q6YTX5_ORYSJ
Q653S9_ORYSJ
miR5564
Q943K7_ORYSJ
DAO
OsJ_045113
Q69AX2_ORYSJ
Q8LR62_ORYSJ
miR167b
GRC2
Q6Z8T9_ORYSJ
Q7XRE7_ORYSJ
A0A0P0Y472
Q8LRC7_ORYSJ
STAR1
NPR2
Q6ZGQ0_ORYSJ
miRN82
Q75LD3_ORYSJ
RPL5
OJ1384D03.13
PP2C30
miRN60
Q2R1N0_ORYSJ
Q6ASU6_ORYSJ
Q6ZLG1_ORYSJ
ADI1
Q6Z7S0_ORYSJ
Q60E66_ORYSJ
Q5JK83_ORYSJ
Q851U1_ORYSJ
PORB
Q8H3I3_ORYSJ
Q688X1_ORYSJ
B9GC17_ORYSJ
Q69RL1_ORYSJ
A3ABE0_ORYSJ
Q336R6_ORYSJ
GAPC1
Q53N83_ORYSJ
Q7XWZ6_ORYSJ
Q5Z790_ORYSJ
Q2QPY6_ORYSJ
miR164
Q6Z6Y4_ORYSJ
Q7XCS3_ORYSJ
Q10IZ3_ORYSJ
Q9LJ01_ORYSJ
miRN58
HEMC
Q69K00_ORYSJ
SNL6
Q7F2X8_ORYSJ
Q0JBE8_ORYSJ
RFS
GLY1-11
RCS1
A0A0P0VBD5
Q6EUD7_ORYSJ
Q6ZCD2_ORYSJ
miR396
Q7EZY8_ORYSJ
Q75M18_ORYSJ
CAB2R
REM4.1
LIR1
OJ2056_H01.33
miR396
Q850T7_ORYSJ
Q6Z7E6_ORYSJ
Q10BA6_ORYSJ
CYP85A1
Q0JD43_ORYSJ
HEM1_ORYSJ
OJ1582_D10.25
Q0IL18_ORYSJ
miR172
Q2QYV1_ORYSJ
Q2QY16_ORYSJ
A0A0P0XWF8
CYP75B3
miRN47
TK
Q7F2G3_ORYSJ
Q75GQ1_ORYSJ
Q5Z8P6_ORYSJ
miR160
miR159
Q5ZDL8_ORYSJ
Q69S79_ORYSJ
Q5TKQ2_ORYSJ
Q5Z624_ORYSJ
OSA15
B7F7E9_ORYSJ
LIP1-2
A0A0P0XP23
LogFC(Badila vs FG1)
-8
-2

A

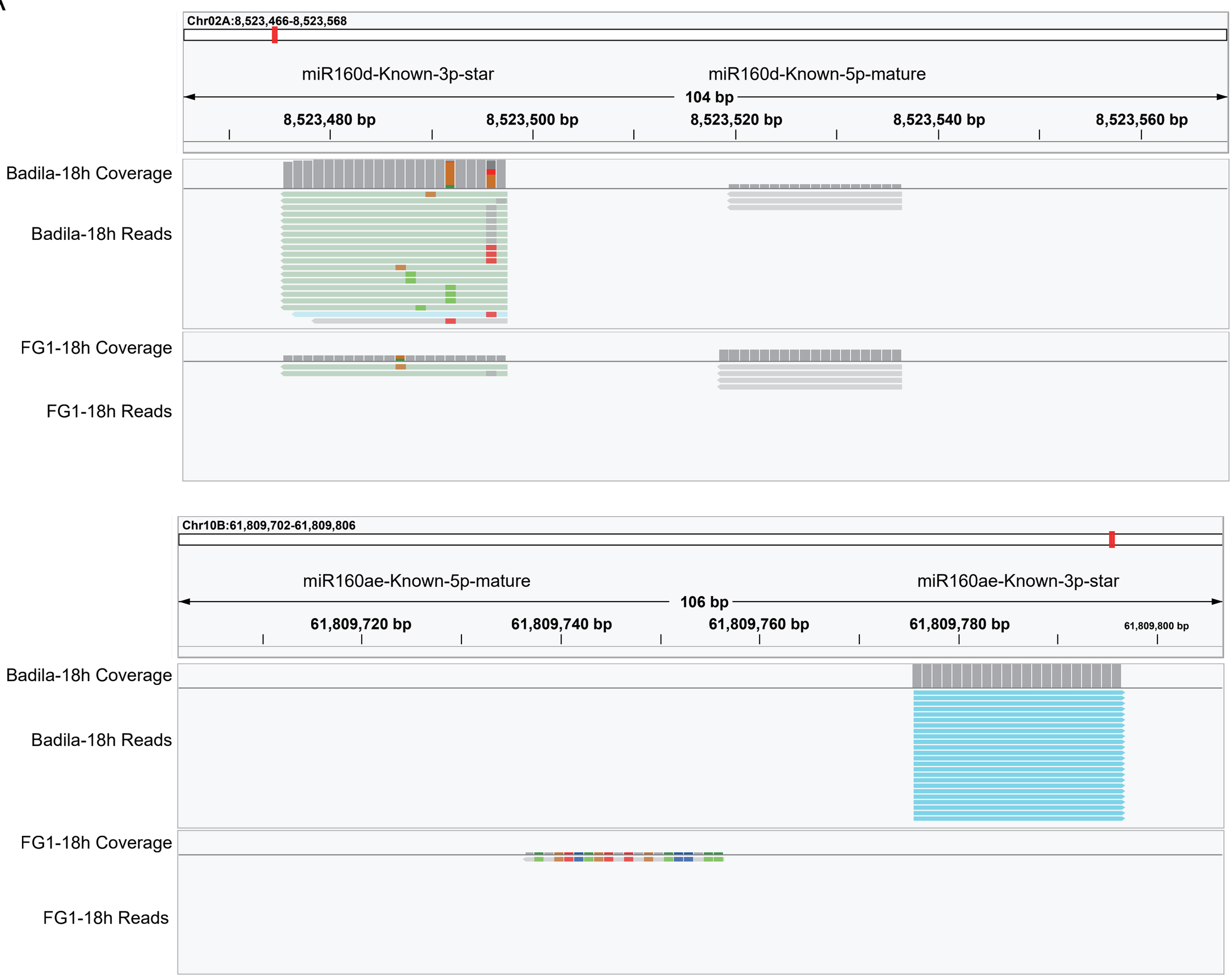
Chr02A:8,523,466-8,523,568
miR160d-Known-3p-star
miR160d-Known-5p-mature
104 bp
8,523,480 bp
8,523,500 bp
8,523,520 bp
8,523,540 bp
8,523,560 bp
Badila-18h Coverage
Badila-18h Reads
FG1-18h Coverage
FG1-18h Reads
Chr10B:61,809,702-61,809,806
miR160ae-Known-5p-mature
miR160ae-Known-3p-star
106 bp
61,809,720 bp
61,809,740 bp
61,809,760 bp
61,809,780 bp
61,809,800 bp
Badila-18h Coverage
Badila-18h Reads
FG1-18h Coverage
FG1-18h Reads

B

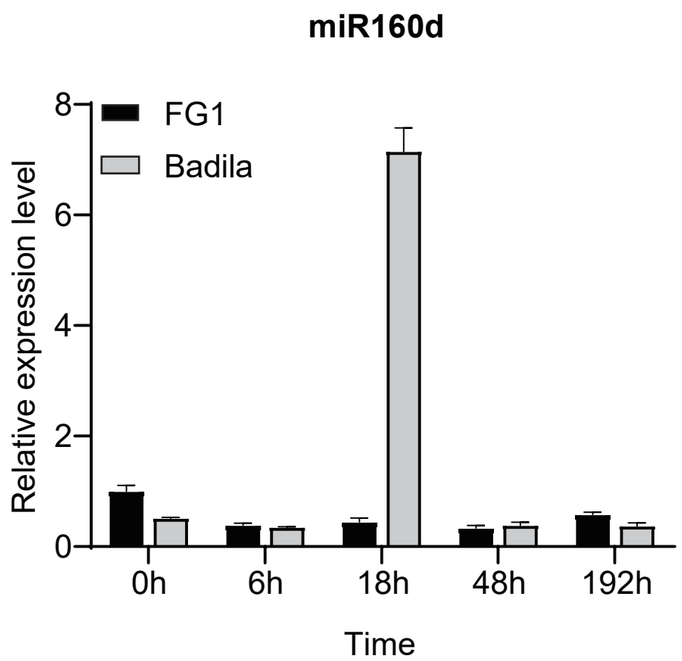
miR160d
FG1
Badila
Relative expression level
0
2
4
6
8
0h
6h
18h
48h
192h
Time

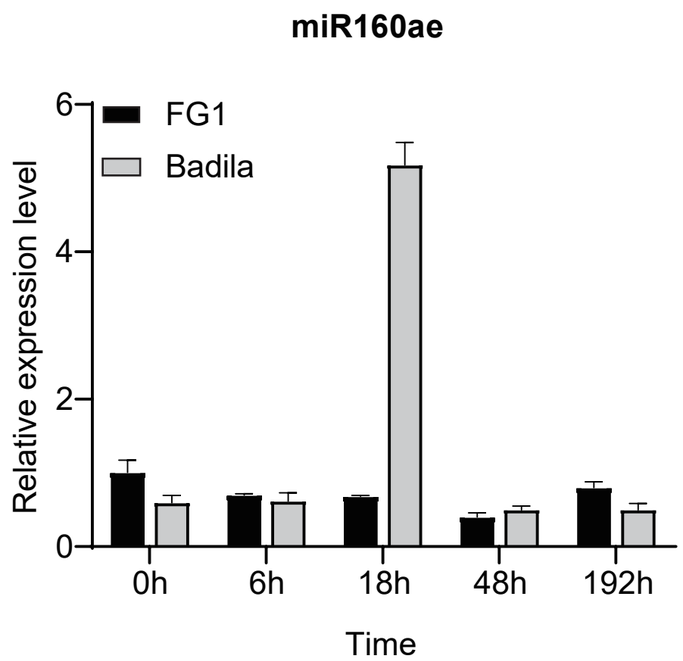
miR160ae
FG1
Badila
Relative expression level
0
2
4
6
0h
6h
18h
48h
192h
Time

C

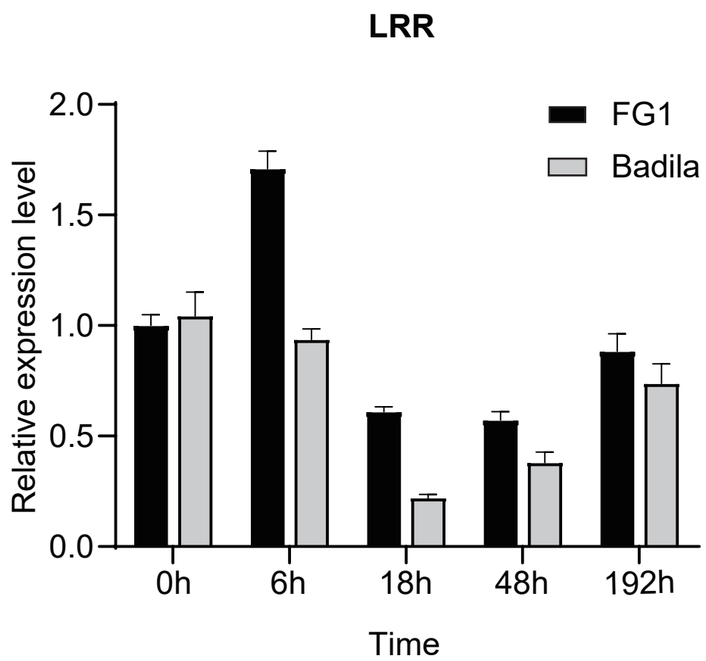
LRR
FG1
Badila
Relative expression level
0.0
0.5
1.0
1.5
2.0
0h
6h
18h
48h
192h
Time

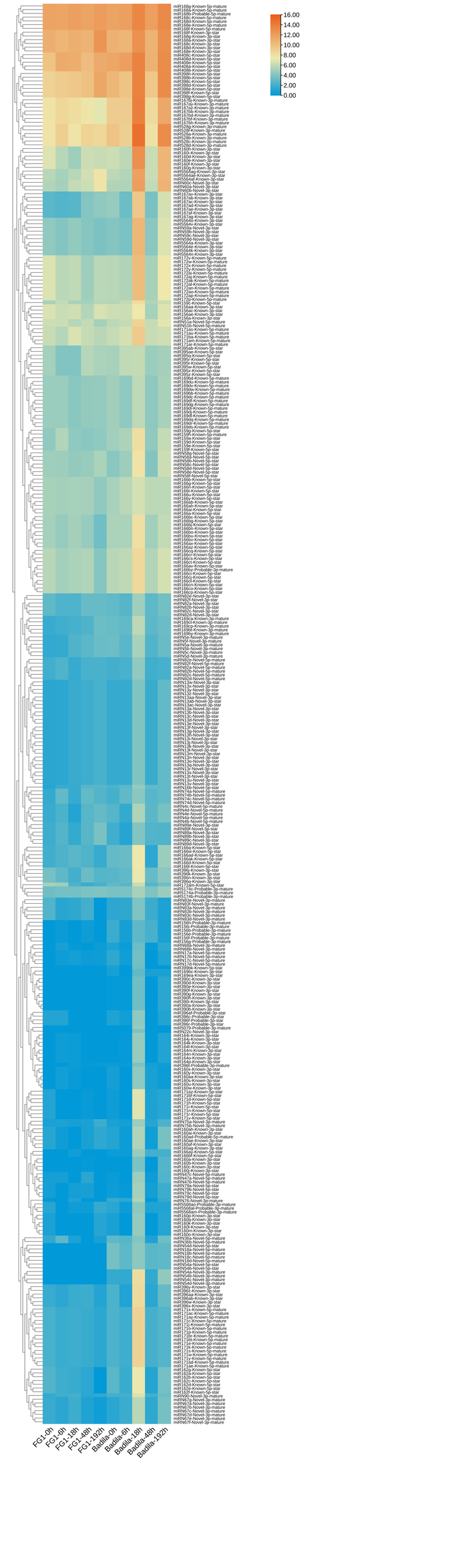
16.00
14.00
12.00
10.00
8.00
6.00
4.00
2.00
0.00
FG1-0h
FG1-6h
FG1-18h
FG1-48h
FG1-192h
Badila-0h
Badila-6h
Badila-18h
Badila-48h
Badila-192h

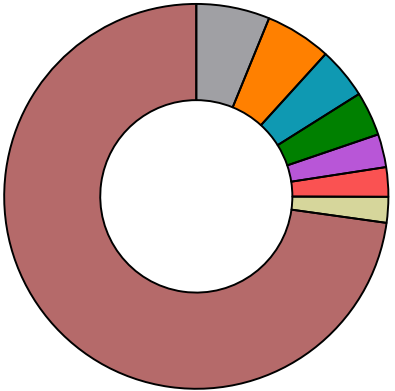

unknown
Protein tyrosine and serine/threonine kinase
Hsp20/alpha crystallin family
Chlorophyll A-B binding protein
EF hand
bZIP transcription factor
Myb-like DNA-binding domain
others